Soft Matter

View Online
Dynamic Article Links

Cite this: DOI: 10.1039/c1sm05594a

www.rsc.org/softmatter

PAPER

Palmitoylation of xanthan polysaccharide for self-assembly microcapsule formation and encapsulation of cells in physiological conditions†

Ana Carina Mendes,[ab] Erkan Türker Baran,[ab] Cláudia Nunes,[c] Manuel A. Coimbra,[c] Helena Sepúlveda Azevedo*[ab] and Rui Luís Reis[ab]

Received 4th April 2011, Accepted 6th June 2011
DOI: 10.1039/c1sm05594a

Hydrophobized polysaccharides have emerged as a promising strategy in the biomedical field due to the versatility to design functional structures through the spontaneous self-assembly in cell-friendly conditions. Based on this concept, xanthan, a bacterial extracellular polysaccharide with potential as encapsulating matrix, was conjugated with hydrophobic palmitoyl groups to obtain an amphiphilic system able to form capsules by self-assembly processes. The conjugation of xanthan was performed at different xanthan/palmitoyl chloride ratios and Fourier transformed infrared, ^{1}H nuclear magnetic resonance spectroscopies, as well as wide angle X-ray diffraction, differential scanning calorimetry were performed to characterize the obtained conjugates. The results showed that the increase in the hydrophobic reactant promoted higher hydrophobic interaction and consequently higher molecular organization. At certain palmitoyl concentrations and through a proper balance between charge repulsion and hydrophobic interaction, the amphiphilic molecules self-assembled into stable capsular hollow structures in the presence of physiological ion concentration and pH. Poly-L-lysine coated microcapsules with an average diameter of 576.6 ± 74 μm and homogenous size distribution were obtained. The morphology revealed by scanning electron microscopy showed microcapsules with two distinct layers. The ability of palmitoyl-xanthan microcapsules to sustain viability and proliferation of encapsulated cells was confirmed by AlamarBlue and DNA assays. These findings suggest the application of palmitoyl-xanthan microcapsules as a potential material for cell encapsulation in cell-based therapies.

1. Introduction

Supramolecular chemistry makes use of non-covalent interactions to achieve the controlled assembly of molecular segments, providing a versatile tool for the spontaneous organization of molecules into stable and functional structures.[1,2] Self-assembly can occur through a change in temperature, pH or ion concentration or be triggered by radiation.[3] Self-assembled structures can mimic aspects of biological systems such as artificial cell membranes, enzymes, or channels which makes this methodology suitable to be applied for bottom-up fabrication of new biomaterial systems that can be used as artificial matrices for cell culture.

Hydrophobized polysaccharides have been extensively studied in the biomedical field due to their capability to spontaneously self-assemble in water into functional nanostructures (bilayer membranes, micelles, tubes and vesicles).[4–8] In general, such hydrophobized polymers consist of a water-soluble main chain, the polysaccharide, carrying a small number of hydrophobic groups. The polysaccharide backbone presents numerous favorable characteristics such as biodegradability, low toxicity and abundance of functional groups for further modification. The amphiphilic nature imparted after hydrophobic modification gives them the possibility to be used in a wide range of applications such as emulsion stabilizers, surface modifiers for liposomes and nanoparticles[9,10] and as drug delivery vehicles.[11,12]

Xanthan gum (Fig. 1A) is an anionic extracellular bacterial polysaccharide with the ability to organize into liquid crystalline phases at specific conditions[13–17] providing an anisotropic nature as a result of the helical structure. This biopolymer was shown to be biocompatible,[17] biodegradable and exhibits gel-like properties, being widely used in food, cosmetic and pharmaceutical industries because of the encouraging reports on safety.[15]

[a]*3B's Research Group—Biomaterials, Biodegradables and Biomimetics, University of Minho, Headquarters of the European Institute of Excellence on Tissue Engineering and Regenerative Medicine, AvePark, 4806-909 Taipas, Guimarães, Portugal. E-mail: hazevedo@dep.uminho.ptmailto; Fax: +351 253 510909; Tel: +351 253 510907*
[b]*ICVS/3B's - PT Government Associate Laboratory, Braga/Guimarães, Portugal*
[c]*QOPNA, Department of Chemistry, University of Aveiro, Campus Universitário de Santiago, 3810-193 Aveiro, Portugal*
† Electronic supplementary information (ESI) available. See DOI: 10.1039/c1sm05594a

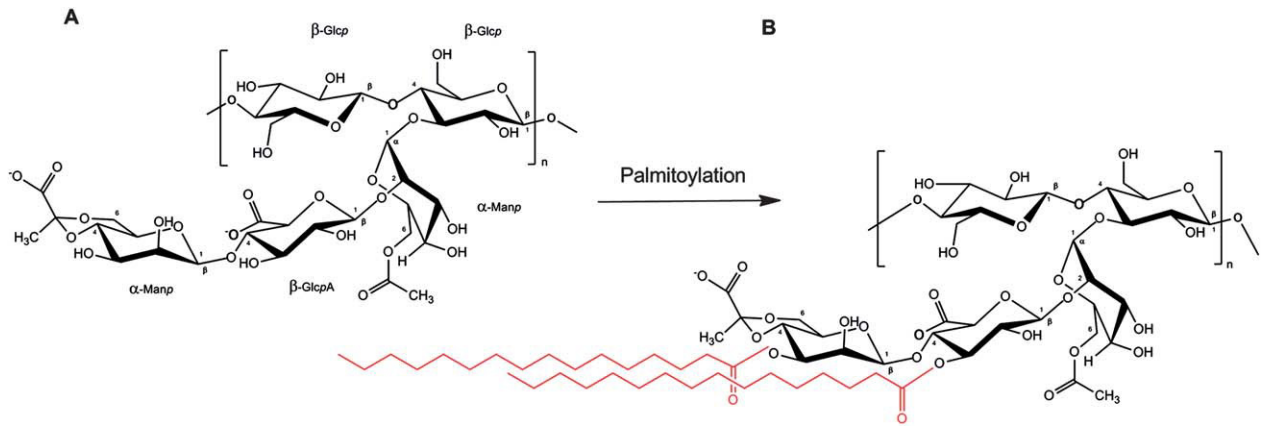

Fig. 1 Chemical structure of xanthan repeating unit (A) and palmitoyl xanthan (B).

Recently, Mendes and co-workers[18] have reported the potential of this biopolymer as cell encapsulation matrix. They demonstrated that stable xanthan microcapsules were generated and encapsulated cells remained viable and were observed to proliferate for prolonged culture periods.

Herein, we present the synthesis of an amphiphilic polysaccharide, in which palmitoyl groups are attached to an anionic polysaccharide chain (xanthan gum) and demonstrate that the amphiphilic polysaccharide (palmitoyl xanthan) is able to self-assemble into capsules in saline solutions. The properties and performance of palmitoyl xanthan microcapsules were studied by exploiting the balance between the hydrophobic and ionic interactions. A second aim of this study was to evaluate the ability of these self-assembled matrices to support the viability, function, and proliferation of encapsulated cells.

2. Materials and methods

2.1 Materials

All chemicals, including xanthan gum from *Xanthomonas campestris*, palmitoyl chloride and Poly-L-Lysine (PLL), were obtained from Sigma/Aldrich unless otherwise indicated. The chemicals were used as received. Characterization of native xanthan (elemental composition, degree of acetylation, molecular weight monosaccharide composition and linkage analysis) is reported in the ESI†.

2.2 Preparation of palmitoyl xanthan (PX)

Xanthan was dissolved in distilled water (1 wt%) at room temperature in a round-bottom glass flask. The polymer solution was placed in an ice-water bath and vigorously stirred using a mechanical stirrer (IKA, Germany). Palmitoyl chloride was then added dropwise at different ratios as shown in Table 1. The mixture was allowed to react under continuous stirring for 23 h. The reaction was stopped by the addition of excess of cold ethanol and filtered. The final product was dried at room temperature until constant mass.

2.3 Characterization of PX

2.3.1 Solubility. The solubility of each palmitoyl-xanthan conjugate was assessed in organic solvents by placing 10 mg of PX in 4 mL of each solvent. The suspension solution was mixed by vortex and placed in a water bath at 37 °C overnight. Solubility was examined visually for any undissolved solute particles.[19] Additional characterization (elemental composition, molecular weight, monosaccharide composition and linkage analysis) of water soluble palmitoyl-xanthan conjugate (PX(X = 1.7P)) is reported in the ESI†.

2.3.2 Fourier transform infrared (FTIR) spectroscopy. The chemical modification of xanthan with palmitoyl was analysed by infrared spectroscopy. Prior to analysis, potassium bromide pellets were prepared by mixing the native xanthan and PXs powder with potassium bromide (KBr, PIKE Technologies, USA) at 1/10 (w/w) PX/KBr ratio. The spectra were acquired on an IR Prestige-21 (SHIMADZU, Japan) spectrophotometer with the average of 32 scans and a resolution of 4 cm^{-1}.

2.3.3 ^{1}H nuclear magnetic resonance (NMR) spectroscopy. The conjugate samples from different ratio of xanthan/palmitoyl chloride were dissolved at a concentration of 1 wt% in deuterated dimethylsulfoxide (d-DMSO). Fully relaxed ^{1}H NMR spectra were acquired in a Varian Unity Plus 300 MHz spectrometer.

2.3.4 Wide angle X-ray scattering (WAXS). The PX conjugates were characterized by the WAXS technique to verify any molecular orientation. Dry powders were transferred to the sample holder and WAXS measurements were performed using a Bruker AXS NanoStar with a HiStar 2D detector with scattering angles from 5 to 60°.

2.3.5 Differential scanning calorimetry (DSC). DSC analysis of PX conjugates was performed in a calorimeter (TA instruments, USA) with a heating program of 10 °C min^{-1} from 10 to

Table 1 Sample designation for each palmitoyl xanthan conjugate

Sample designation	Xanthan/ mmol	Palmitoyl chloride/ mmol	Xanthan/palmitoyl chloride ratio/mol mol^{-1}
PX(X = 0.50P)	0.58	1.18	0.50
PX(X = 0.75P)	0.58	0.78	0.75
PX(X = 1.40P)	0.58	0.42	1.40
PX(X = 1.70P)	0.58	0.35	1.70

200 °C under nitrogen at a flow rate of 20 cm^3 min^{-1}. DSC was also carried out for the water soluble conjugate sample (PX(X = 1.7P)) after extraction with excess chloroform (three times) to remove traces of free palmitic acid (ESI†).

2.3.6 Circular dichroism (CD). CD was used to study the effects of palmitoylation on the secondary structure of native xanthan. PX(X = 1.7P) and native xanthan were dissolved in ultrapure water overnight at a concentration of 0.1 wt%. The measurements were performed in a stopped-flow circular dichroism spectropolarimeter (PiStar-180, Applied Photophysics, UK) at 25 °C using Quartz cells with a 0.1 cm path length. The spectra were recorded from 300 to 180 nm with a scan rate of 100 nm min^{-1} and are an average of five accumulations.

2.3.7 ζ Potential measurements. ζ Potential measurements were performed using a Zetasizer NanoZS Instrument (ZEN 3600, Malvern Instruments, Worcestershire, UK). Prior the analyses, PX(X = 1.7P) and xanthan solutions were prepared at a concentration of 0.1 wt% and their pH was adjusted to 5, 6, 7 and 8 using 0.1 M HCl, and 0.1 M NH_4OH. The solutions were filtered using a pyrogen free 0.45 μm disposable membrane filter (Schleicher and Schuell Bioscience, Germany).

2.3.8 Scanning transmission electron microscopy (STEM). STEM samples of xanthan (control) and water-soluble PX conjugate were prepared by placing one drop of the polymer solution (0.1 wt%) onto a 300 mesh copper grid coated with carbon film, followed by 1% (w/v) of uranyl acetate (Electron Microscopy Sciences) staining for 3 min. The samples were analyzed and photographed using a ultra-high resolution analytical scanning electron microscope (HR-FESEM Hitachi SU-70).

2.4 Microcapsule formation by self-assembly and characterization

To study the capability of the palmitoyl-xanthan conjugates to form suitable capsules for cell encapsulation, we have selected PX(X = 1.7P) conjugate taking into account its solubility in aqueous solutions. Various concentrations of PX(X = 1.7P) solutions (1–3%) were tested for microcapsule preparation. 1% solution provided smooth and spherical microcapsules and this concentration was further used in the subsequent studies. PX (X = 1.7P) was dissolved in HEPES buffer solution (55 mM, pH 7.4, Sigma) supplemented with 0.1 M $CaCl_2$ and 0.15 M NaCl at concentration of 1 wt% and further sterilized by UV light for 20 min in a laminar flow cabinet. Capsules were formed by extrusion of the polymer solution from a disposable plastic syringe with a 2.5 G diameter needle into a flask containing PBS.

2.4.1 Microcapsule morphology: scanning electron microscopy (SEM). Previous to SEM observation, the capsules were fixed subsequently for 1 h with formaline 3.7% and 3% v/v of glutaraldehyde (Electron Microscopy Sciences) in PBS. The samples were further dehydrated in graded ethanol series (20, 50, 60, 70, 80, 90 and 100%) followed by immersion in 100% hexamethyldisilazane (HMDS, Electron Microscopy Sciences). The specimens were transferred and mounted on aluminium stubs and allowed to dry at room temperature. Microcapsules were cut in half to expose the membrane cross-section and the internal surface of microcapsules. Prior to observation, they were sputter coated with Pt/Pd target (80/20) generating a thin film with 6 nm of thickness (208 HR High Resolution Sputter Coater, Cressington). The microcapsules were imaged on an ultra-high resolution field emission gun scanning electron microscope (FEG/SEM, FEI Nova 200 NanoSEM).

2.5 Cell encapsulation and culture

To validate the utility of PX as cell encapsulating matrix, we carried out cell culture studies within the PX microcapsules. The murine ATDC5 chondrocyte cells were cultured in basic medium, consisted of Dulbecco's Modified Eagle's Medium (DMEM, Sigma-Aldrich) with phenol red, supplemented with 10% fetal calf serum (FCS, Biochrom AG), 5 mM L-glutamine (Sigma) and 1% of antibiotic–antimycotic mixture (Sigma) and maintained at 37 °C in a humidified atmosphere of 5% CO_2. The medium was replaced every two days. At passage 9, cells were detached with trypsin/EDTA and counted in a hemacytometer for encapsulation. A cell suspension (5×10^6 cells per mL, 0.5 mL) was mixed with PX(X = 1.7P) solution (1.5 mL, 1 wt% final concentration). The cells were encapsulated into the PX (X = 1.7P) matrix using a novel micro-droplet generator developed in our group as previously reported[18,20] (Fig. 2). Briefly, an autoclavable tubing (Novosil, Fisher Scientific) with 1 mm internal diameter was punctured with a blunt end needle (12 G) in a vertical position and sealed with a silicone glue. This assembly was then connected to a peristaltic pump (Ismatec, Switzerland) for perfusion of mineral oil and syringe pump (Aladdin WPI, England) for gel–cell injection in a sterile laminar flow cabinet. One end of the tubing was connected to an oil reservoir and the other end to a glass collector, where the microdroplets of gels can be self-assembled in a PBS solution. The operation rates of peristaltic and syringe pump were set at 0.35 mL min^{-1} and 0.50 μL min^{-1}, respectively. The microcapsules were stirred in collection vessel for 15 min and then transferred into 0.1 wt% poly-L-lysine solution and stirred for 10 min. The coated microcapsules were transferred into tissue culture wells with DMEM and cultured in standard conditions (37 °C and 5% CO_2) for 1, 7, 14 and 21 days. The medium was exchanged every 2 days. In addition, for average microcapsules size determination, the images of microcapsules from a bright field light microscope (AXIOVERT 40 CFL, Zeiss, Germany) were analyzed by an image analyzer software (Image J, version 1.38, National Institute of Health, USA).

2.5.1 Cell viability—live/dead cell assay. Calcein AM (Sigma) solution (2/1000, v/v) was prepared in DMEM medium without FCS and phenol red. Propidium iodide (PI, Molecular Probes, Invitrogen) solution was prepared by mixing 2 μL PI (1 mg mL^{-1}) with 20 μL (1 mg mL^{-1}) RNase A (USB corporation) and 2 mL PBS. The microcapsules with encapsulated cells and controls (without cells) were collected from the culturing plates and incubated with calcein-AM and propidium iodide solutions at 37 °C for 10 min protected from light. Microcapsules were then observed under fluorescent microscopy using an Axioplan Imager Z1m microscope (Zeiss, Germany).

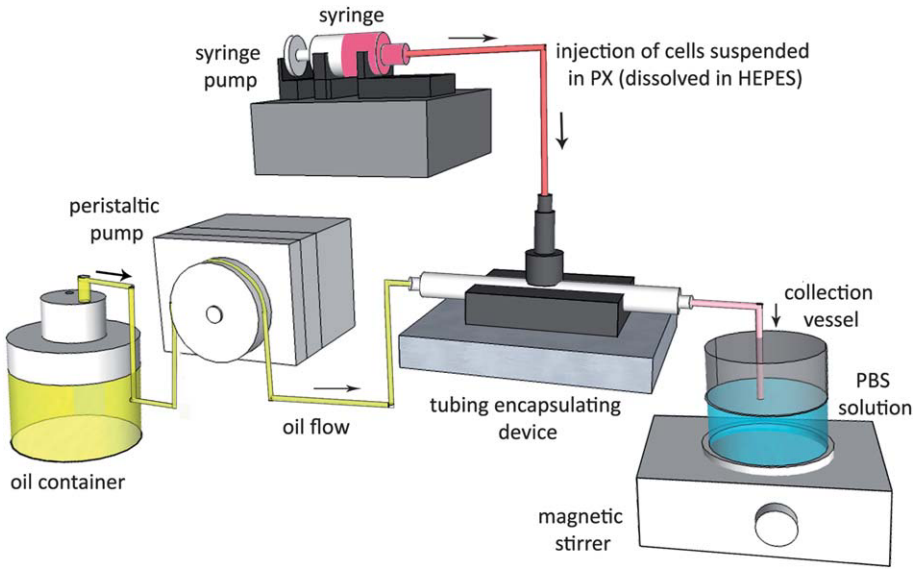

Fig. 2 Schematic of the set-up for cell encapsulation showing details of the micro-droplet generator. A solution of palmitoyl xanthan, with or without cells, was injected into a stream of mineral oil resulting in the formation of spherical droplets and a water-in-oil emulsion due to the immiscibility of the two phases. The polymer microdroplets in oil were then carried into a gelling inducer solution (phosphate buffer solution, PBS). In PBS, the palmitoyl xanthan droplets self-assemble into capsular gel structure. The hollow capsules were then collected and treated with poly-L-lysine to strengthen the outer surface of the microcapsules.

2.5.2 Metabolic activity of encapsulated cells—AlamarBlue® assay. The metabolic activity of encapsulated cells over time was assessed using the AlamarBlue® assay (AbD Serotec). AlamarBlue® was added (10% of the volume of the well) to each well containing the encapsulated cells and the plate was incubated at 37 °C for 20 hours protected from light. After incubation, aliquots were taken and transferred to a 96-well plate and the absorbance was measured at 570 and 600 nm on a microplate reader (BIO-TEK, Synergie HT, USA). The percentage of reduced AlamarBlue® was calculated according to the manufacturer instructions.

2.5.3 Cellular proliferation assay—DNA quantification. ATDC5 proliferation within the capsules was determined using a fluorimetric DNA quantification kit (PicoGreen, Molecular Probes, Invitrogen). For this purpose, the samples collected at days 1, 7, 14 and 21 were washed twice with sterile PBS (Sigma, USA) solution and placed in 1 mL of ultra-pure water. Capsules with and without cells were stored at −80 °C until further analysis. Prior to DNA quantification, samples were thawed and broken by pipetting up and down using a syringe with a needle to cause material disruption and facilitate DNA extraction. 28.7 μL aliquots and standards (0–2 mg mL^{-1}) were transferred to an opaque 96 well plate. Then 71.3 μL of PicoGreen solution and 100 μL of Tris–EDTA buffer were added. Standards and samples were prepared in triplicate. The plate was incubated for 10 min in the dark and the fluorescence was measured using an excitation wavelength of 485 nm and emission of 528 nm. DNA amounts were calculated from the calibration curve.

2.5.4. Statistical analysis. The results of DNA quantification and cell viability are expressed as a mean ± standard deviation with $n = 3$ for each group. Statistical significance of differences was determined using the unpaired Student's *t*-test multiple comparison procedure at a confidence level of 95% ($p < 0.05$).

3 Results and discussion

The synthesis of palmitoyl xanthan was accomplished in a single-step reaction (Fig. 1). Hydrophobically modified xanthans were prepared with different hydrophobic modification ratios (Table 1). The degree of substitution per hydroxyl group for the highest xanthan/palmitoyl chloride molar ratio (PX(X = 1.7P) was not very high (1.26%, ESI†).

3.1 Solubility analysis

The solubility of the palmitoyl/xanthan conjugates was tested in polar protic and aprotic solvents (Table 2). PX(X = 1.7P) palmitoyl xanthan is the only conjugate that showed solubility in water which is a basic requirement for cell encapsulation in aqueous physiological buffer solutions. As shown in Table 2, all the PX conjugates are soluble in DMSO, but PX(X = 1.4P) and PX(X = 1.7P) are also soluble in THF and PX(X = 0.75P) also dissolves in DCM. The conjugates soluble in organic solvents could be further used as biomaterials, in particular for the production of nano- and microparticles by using an emulsion and solvent extraction/evaporation methods. In our study, however, the PX(X = 1.7P) conjugate was selected as suitable conjugate for microencapsulation of mammalian cells as it provides an amphiphilic and self-assembly property in physiological pH and ionic strength.

3.2 FTIR spectroscopy

The FTIR spectrum (Fig. 3A) of native xanthan shows a carbonyl (C═O) band at 1725 cm^{-1} corresponding to acetate

Table 2 Solubility of P*X* conjugates in various polar aprotic (THF, DCM, acetone, DMSO) and protic (ethanol and water) solvents

Sample designation	Tetrahydrofuran (THF) (DEC: 7.5)	Dichloromethane (DCM) (DEC: 9.1)	Acetone (DEC: 21)	Dimethyl sulfoxide (DMSO) (DEC: 46.7)	Ethanol (DEC: 16.8)	Water (DEC: 80)
PX(X = 0.50P)	Swelled	Swelled	—[a]	Dissolved	—[a]	—[a]
PX(X = 0.75P)	Swelled	Dissolved	—[a]	Dissolved	—[a]	—[a]
PX(X = 1.40P)	Dissolved	Swelled	—[a]	Dissolved	Swelled	—[a]
PX(X = 1.70P)	Dissolved	Swelled	—[a]	Dissolved	Swelled	Dissolved

[a] Not dissolved, nor swelled. DEC: dielectric constant.

groups of an inner mannose unit. At 1606 cm^{-1}, the characteristic band of carboxylate of pyruvate group and glucuronic acid appears.[17] Spectra of modified xanthans show a shift in the carbonyl band towards 1700 cm^{-1}. These changes may indicate the presence of additional ester groups and suggest that palmitoyl groups substituted the hydrogen atoms of hydroxyl groups in xanthan. It can also be noted the appearance of two absorption bands at 2914 and 2846 cm^{-1}, attributed to CH_3 and CH_2 vibrations from palmitoyl chains.[21] The spectra show that the intensity of absorption bands is proportional to the palmitoyl content added during the modification.

3.3. ^{1}H NMR spectroscopy

^{1}H NMR spectra of palmitoyl xanthans (Fig. 3B) show peaks from the protons corresponding to the palmitoyl chain at 0.858 ppm (terminal methyl group), 1.062 ppm (13 methylene groups), 1.234 ppm (β-methylene group) and 2.380 ppm (α-methylene group)[22] whose intensities are proportional to the amount of reacted palmitoyl.

3.4 WAXS

To verify possible molecular organization after palmitoylation, we carried out WAXS experiments. Diffractograms of xanthan and palmitoyl/xanthan ratios (Fig. 4A) show the appearance of new peaks after modification, demonstrating that the native structure of xanthan has been modified after palmitoylation and this modification has induced a certain molecular organization. As expected, the peak intensity of palmitoyl xanthan increased proportionally with the feed ratio of palmitoyl chloride reactant (from PX(X = 1.7P) to PX(X = 0.5P)). This fact may be attributed to the higher amount of aliphatic chains (palmitoyl groups) that promotes higher hydrophobic interaction and consequently higher organization degree at a structural level. Bragg's law gives the periodic distance, *d*-spacing values, that may correspond in this specific case to the distance for regularly molecular packing. Particularly, if the self-assemblies form bilayered structures with a same orientation, the *d* value should give the relative distance for the interdigitated hydrophobic interaction between alkyl chain groups, which is related to the hydrophobic interaction. Considering similarities between the main peaks, and comparing peak intensities as well as *d*-spacings (Table 3), the intensities, as mentioned before, increase with an increase in the amount of palmitoyl chains due to the increase in hydrophobic interactions. Nevertheless, in all the samples, the distances between alkyl groups (*d*-spacing) do not change significantly with the amount of reacted palmitoyl chloride (Table 3) indicating that the arrangement of molecular packing should be the same independent of the intensity of hydrophobic forces (or amount of palmitoyl chains used in such reactions).

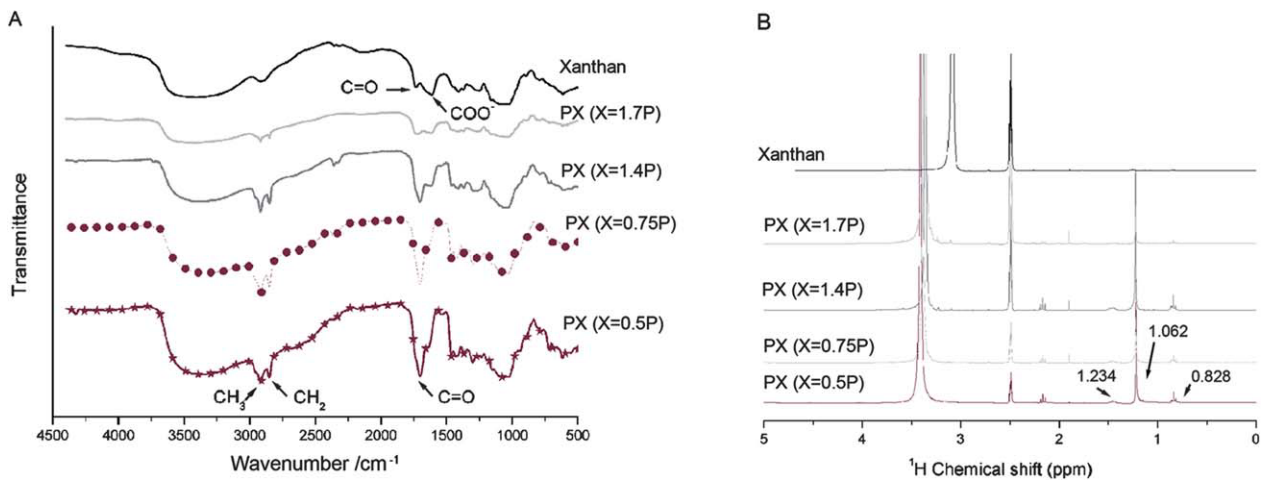

Fig. 3 (A) FTIR and (B) ^{1}H NMR spectra of native xanthan and palmitoyl xanthan with various degrees of modification [PX(X = 0.5P), PX(X = 0.75P), PX(X = 1.40P) and PX(X = 1.70P)].

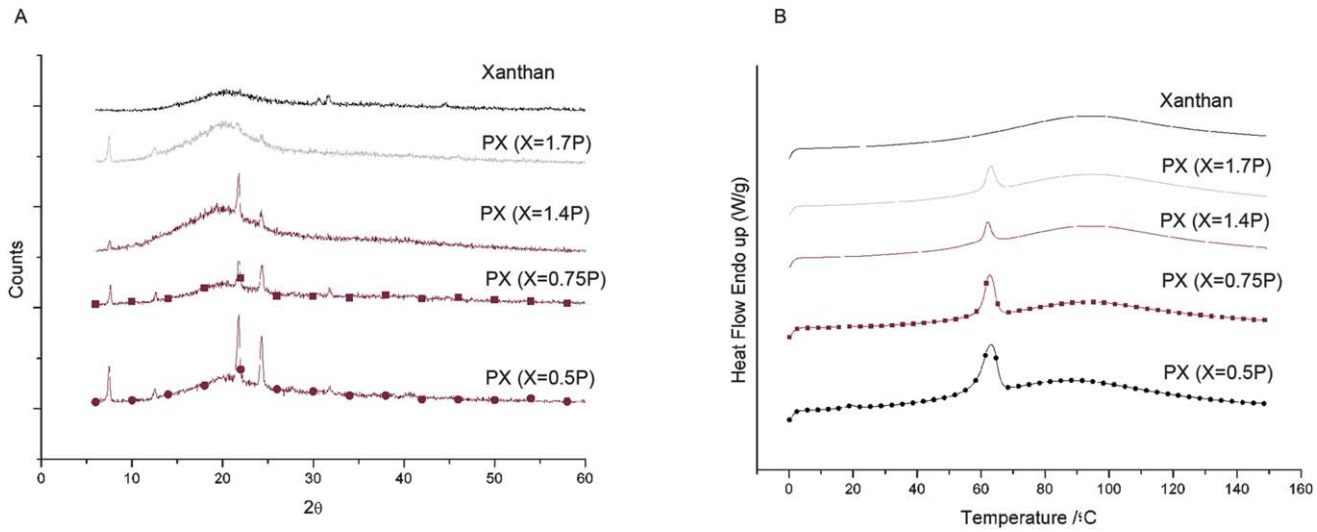

Fig. 4 (A) WAXS spectra and (B) DSC thermograms of xanthan and palmitoyl xanthan(s).

The main peaks of conjugate materials were detected at 21.8 and 24.32 2⊖ values, which correspond to 4.15 and 3.74 Å respectively (Table 3). The found *d*-values indicate that the ordered structures are near one and a half and two palmitoyl chain lengths, as Benages *et al.* observed in pure nanocrystals of palmitic acid (about 2 Å).[23] As the palmitoylation was increased, the relative intensity ratio of 3.74 Å/4.15 Å was higher, showing that the palmitoyl chains are interacting more with opposite chains, which may induce stacking between aliphatic chains and shorten the packing distance.

3.5 DSC analysis

The DSC curves of palmitoyl xanthan (Fig. 4B) show one endothermic phase transition at 61 °C which is less intense as the amount of palmitoyl added to reaction is lower. In the DSC curve of native xanthan, no relevant transition was observed. These observations are corroborating the WAXS results. Such behaviour may be attributed to the increased hydrophobic interactions provided by the higher amounts of reacted palmitoyl that will supply a molecular rearrangement and consequently induce intermolecular organization.

Table 3 Wide angle X-ray diffraction data of palmitoylated xanthan in various conjugation ratios

Sample designation	Angle 2⊖	*d*-Spacing/Å
PX(X = 0.50P)	7.48	11.82
	12.56	7.09
	21.80	4.15
	24.32	3.74
	31.84	2.92
PX(X = 0.75P)	7.52	11.84
	12.60	7.06
	21.84	4.14
	24.28	3.74
	31.76	2.92
PX(X = 1.40P)	7.52	11.84
	21.80	4.15
	24.28	3.74
PX7(X = 1.7P)	7.32	12.12
	12.36	7.19
	21.60	4.18
	24.44	3.71
Xanthan	31.60	2.94

3.6 Molecular conformation—CD spectroscopy

CD spectroscopy is a suitable technique to predict molecular conformation in the liquid state. We used CD to investigate changes in the molecular structure of xanthan after palmitoylation. CD analyses of xanthan and PX(X = 1.7P) were performed at 25 °C in water. The spectrum of both polymers (Fig. 5A) showed an increase in the peak height with maximum absorption wavelength at 196 nm (ordered state) and a decrease in the minimum with displacement at higher wavelengths at 220 nm (disordered state). Despite both materials presenting similar CD signatures, in PX(X = 1.7P) the difference in absorption of left-hand and right-hand circularly polarized light is more accentuated, allowing us to deduce that the introduction of such hydrophobic tails promotes a soft disruption of the organized structure. Considering that the palmitoylation was performed at low temperature (~0 °C), at which an ordered helicoidal structure on native xanthan is present, it is more probable that the palmitoyl chains reacted with the hydroxyl groups of the trisaccharide side chain due to the difficulty to access the internal primary structure. Previously, the ordered conformation of xanthan was investigated thoroughly and indicated that native xanthan involves single or double helix structure and the solid state forms a helical structure with 5-fold symmetry.[24] As a result of conjugation of palmitoyl chains to hydroxyl groups, the disruption of hydrogen bonds, which are necessary for helicoidal structure formation, can be expected.

The native structure of xanthan has been reported in several studies which showed that this biopolymer could be stable when assuming helical structure,[16] being also temperature dependent.[13,15] According to Lim and co-workers[25] for concentrations above 1 wt%, xanthan may self-assemble into liquid crystalline regions. However, at around 0.5%, the structure is not liquid crystalline in nature but presents networks formed by self-organization provided by hydrogen bonding. It has been studied

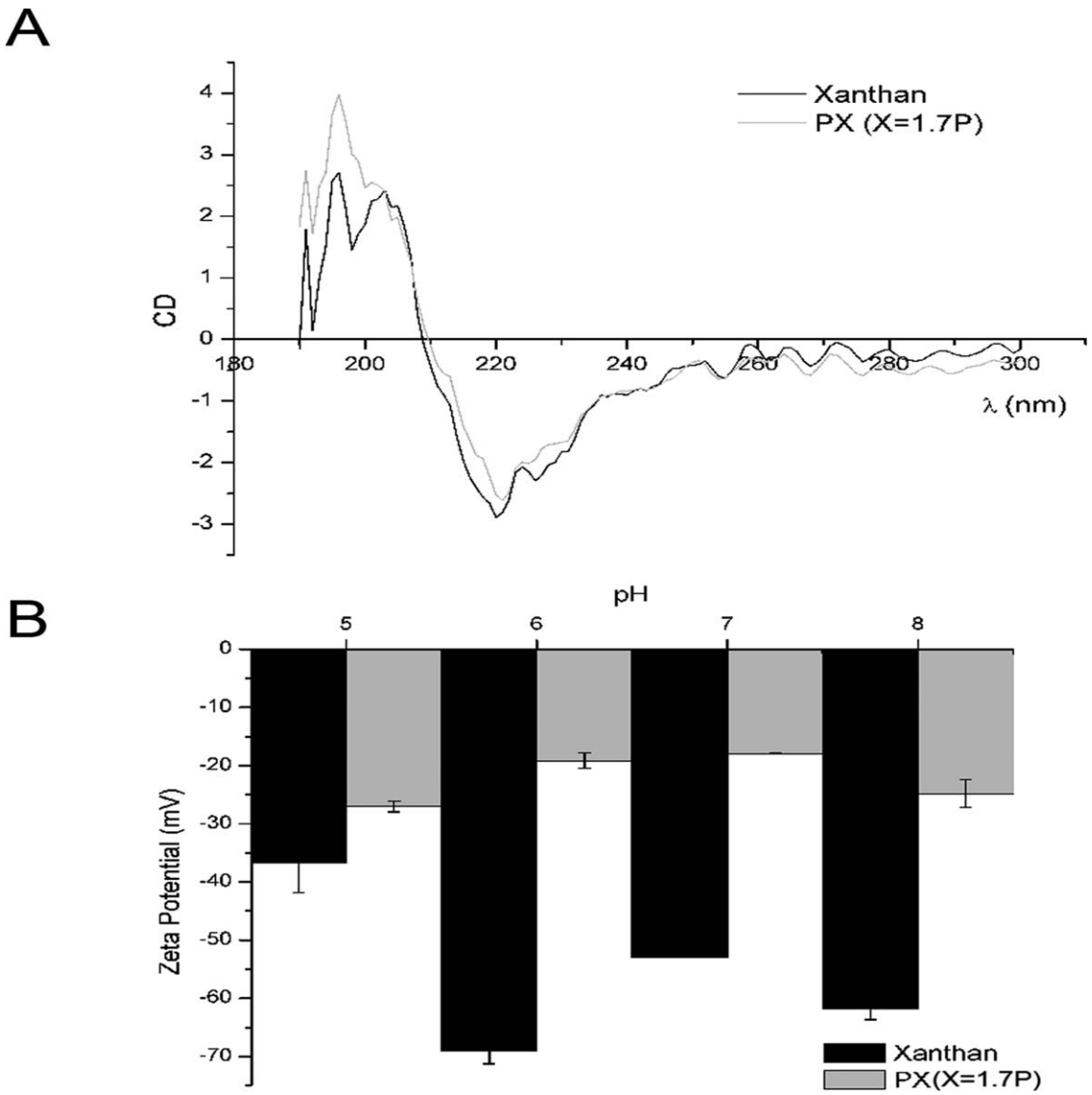

Fig. 5 (A) CD spectra of xanthan and PX(X = 1.70P) solutions (0.1 wt%) in distilled water. (B) ζ Potential measurements of xanthan and PX(X = 1.70P) xanthan conjugate in aqueous solution as a function of pH.

before that xanthan forms gels in the presence of salts and those have the ability to stabilize the ordered conformation.[13,15,16]

3.7 ζ Potential measurements

The electrical charge (ζ-potential) of polymers is dependent on several factors such as the pH, polymer conformation, and polymer concentration. Fig. 5B presents the ζ potential of PX(X = 1.7P) and native xanthan as a function of pH. As the pH increases, the carboxylic groups of xanthan become deprotonated (negatively charged) and thus an increase in the negative ζ potential is expected. At low pH (pH 5), PX(X = 1.7P) exhibits a ζ potential value of −26 mV, which becomes less negative as the pH increases, reaching the minimum at pH 7 (−17 mV) and then increases again at pH 8. The lowest charged state at pH 7 may be due to a kind of stereochemical protection of carboxylic groups provided by the palmitic groups and consequently less sensitive to pH changes. The repulsion between charged groups is expected to be lower and this can enhance hydrophobic action between alkyl chains. Similarly, a recent study showed that a rapid hydrogelation of *N*-palmitoyl chitosan occurred through a proper balance between charge repulsion and hydrophobic interaction at its environmental pH within a narrow range (pH 6.5–7.0).[22] Given these preliminary results, pH 7 was considered for the self-assembly of the amphiphilic conjugate.

3.8 STEM analysis

In order to investigate the supramolecular rearrangement of palmitoyl xanthan in physiological conditions, namely in an ionic strength of 0.9% NaCl and at pH 7.4, the cast solutions of conjugate were analyzed with a scanning transmission electron microscope after negative staining with uranyl acetate. The conjugate which was not exposed to any ionic solution and dissolved in distilled water showed random, thin, fibrous network

structures as seen by STEM micrographs (Fig. 6). This fibrous network structure was also evident when the conjugate was dissolved in HEPES buffer containing 0.1 M $CaCl_2$ and 0.15 M NaCl. In that case, however, the thickness of fibrous structures was increased as determined by STEM micrographs at various magnifications. When the palmitoyl xanthan solution was incubated in PBS similar to microcapsule preparation, on the other hand, lamellar structures were observed instead of fibrous networks. The magnified STEM images clearly show that the assembled structures were formed in an angular and lamellar morphology. In addition, the STEM micrographs of native xanthan did not indicate any visible ultra-structures which can interact with negative staining as seen in the micrographs. Those results may indicate that there were light supramolecular organizations of palmitoyl xanthan molecules in aqueous environment without ions. This was even more pronounced in HEPES buffer solution by the increased size of fibrous structures but still it was not sufficient for a major hydrophobic interaction resulting in stable assemblies. The aggregation of PX molecules in the ionic and pH milieu provided by PBS and the observation of lamellar structures were supporting the hypothesis that a major hydrophobic transition occurred in physiological conditions.

3.9 SEM analysis

As the first attempt to produce capsules, we tried to extrude 1 and 3 wt% xanthan in PBS. Although capsules were able to be formed, they were not stable as they started to dissolve. Aiming to improve the stability of xanthan capsules, the procedure described previously was performed and successful with PX(X = 1.7P), resulting in the hollow capsules shown in SEM micrographs (Fig. 7A). SEM analysis of PX(X = 1.7P) microcapsules

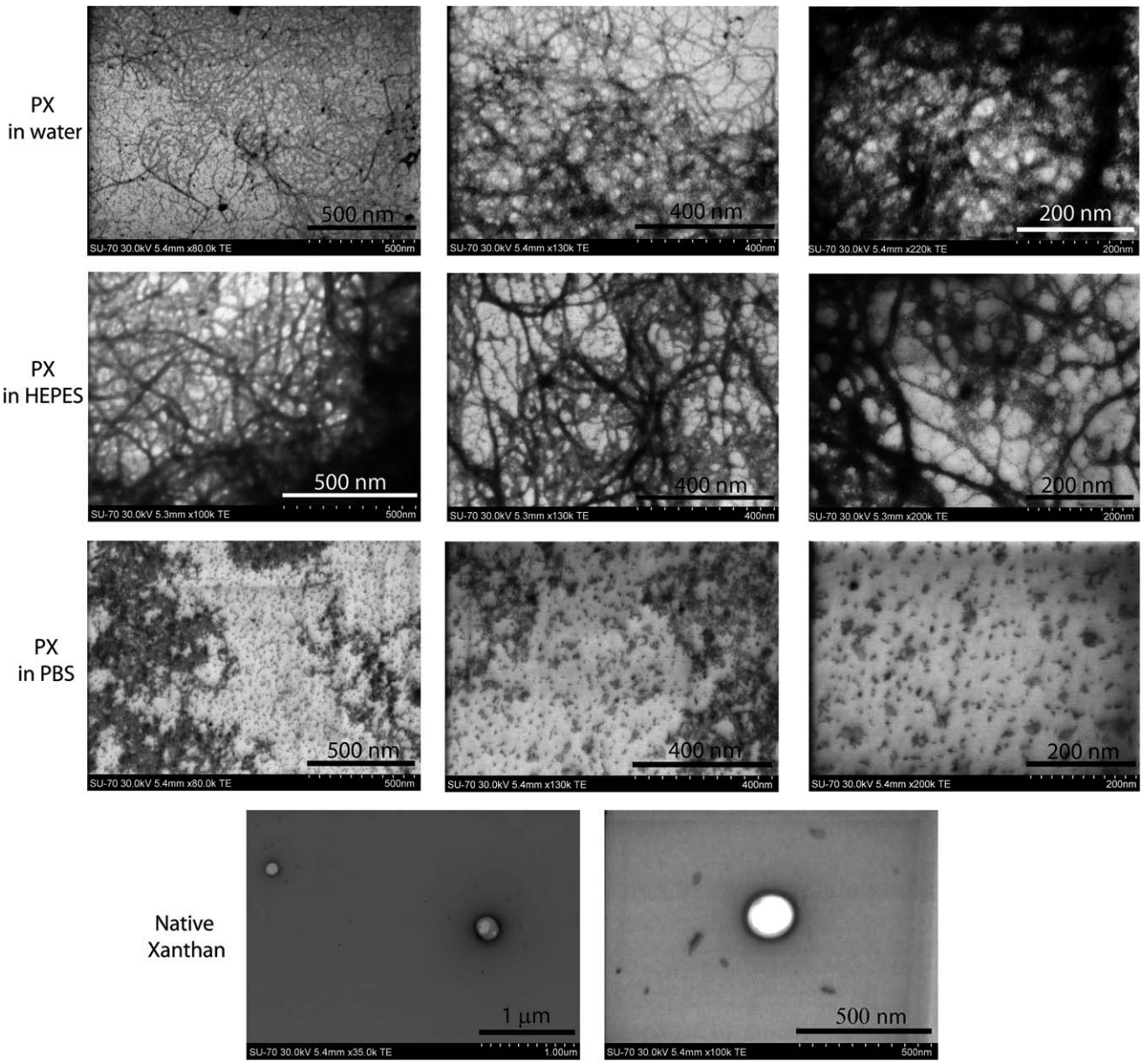

Fig. 6 STEM images of palmitoyl-xanthan in 0.1 wt% solution. The samples were negatively stained with 1% (w/v) uranyl acetate.

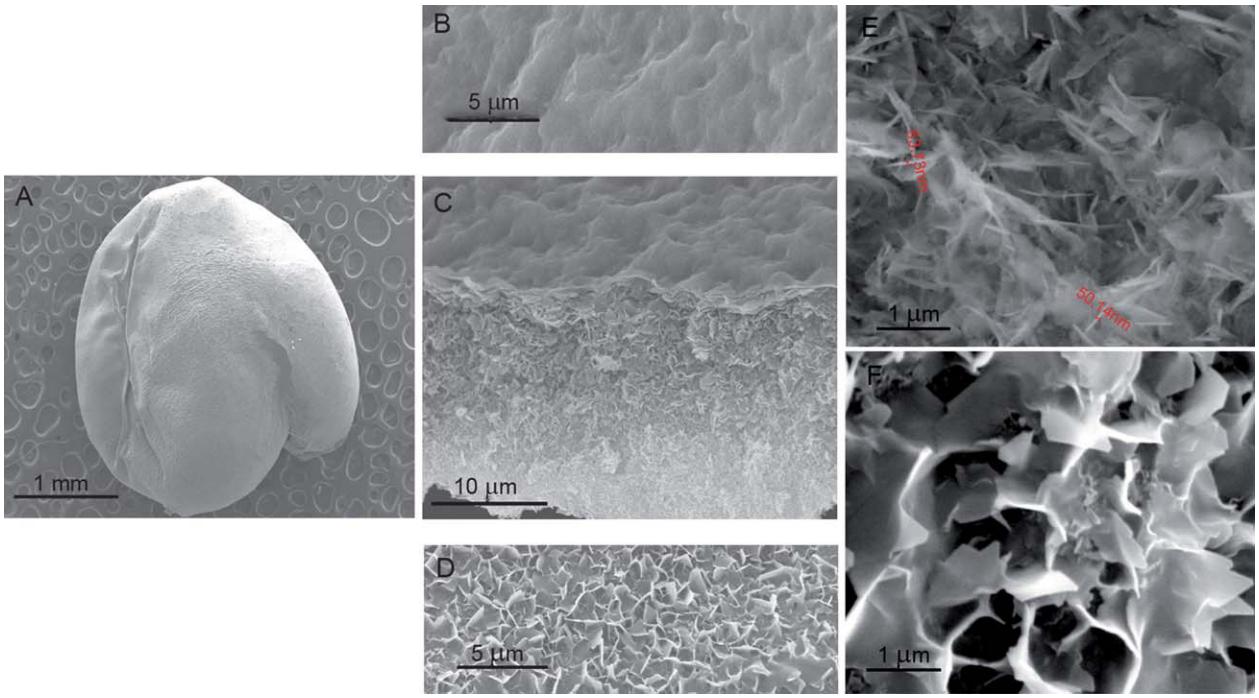

Fig. 7 SEM images showing the overall structure of PX(X = 1.70P) capsules performed manually (A), cross-section of microcapsule membrane (C) and the microstructure of the capsule internal (B) and external surface (D). Magnified images revealing morphological details of the external surface of PX(X = 1.70P) capsules (E and F).

has indicated that the external wall structure was constituted of nano-lamellae which are overlapping each other with a layer thickness of about 52 nm as observed on the surface and inside the wall cross-section (Fig. 7C–F). Based on organization of ultrastructures revealed by SEM, it can be hypothesized that salt addition results in the screening of electrostatic repulsion and the hydrophobic interaction between conjugated alkyl chains become the dominating forces leading to molecular packing (Fig. 8). The internal calcium in the gel must diminish repulsion forces between carboxyl groups by ionic bridge formation and subsequently, the monovalent cations provided from PBS must interact with the polar groups of the polysaccharide backbone by decreasing their solvation with water molecules. As a result of those interactions, the hydrophobic forces between alkyl chains become a dominant force and a self-organization of molecules resulted in multilayered lamellar structures. Those layered

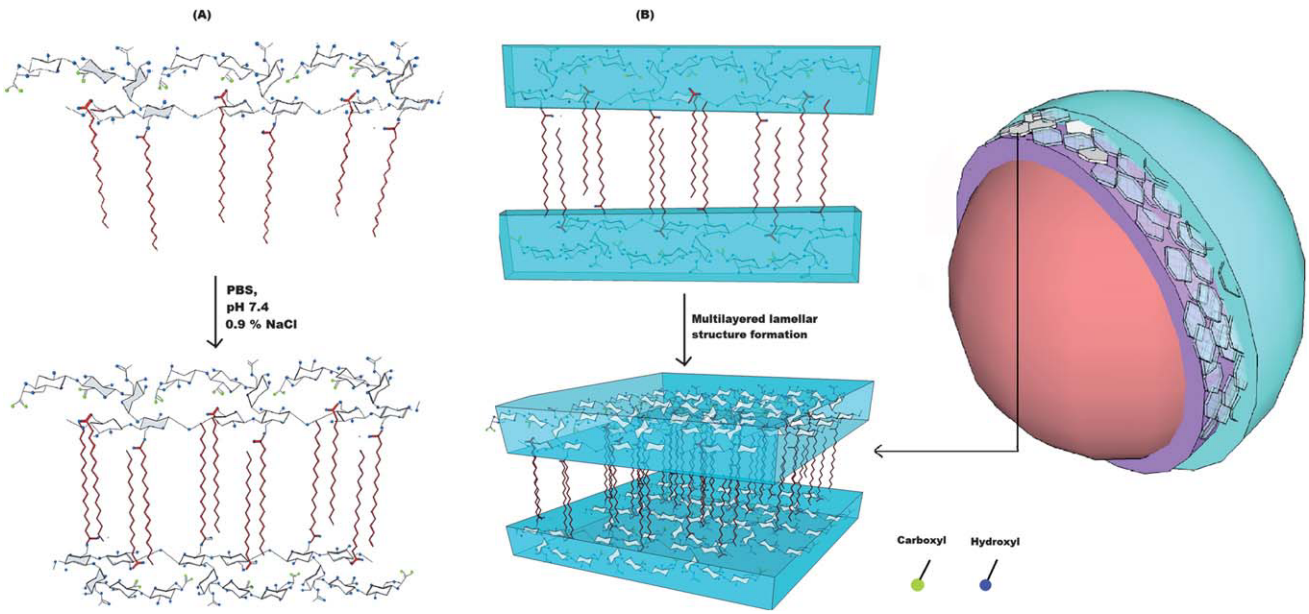

Fig. 8 Schematic depiction of microcapsule formation mechanism by PBS induced self-assembly of palmitoyl-xanthan amphiphile molecules (A) and the mechanism of microcapsule formation (B) by hydrophobic forces.

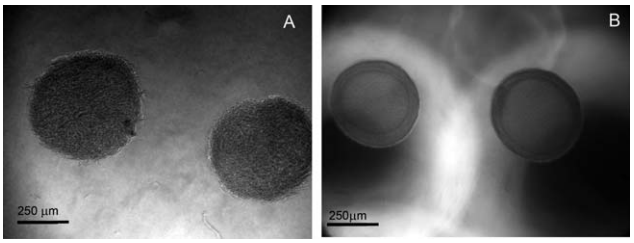

Fig. 9 Bright field light microscopy images of PX(X = 1.70P) microcapsules uncoated (A) and coated (B) with poly-L-lysine (external layer) obtained using the micro-droplet generator.

structures can further aggregate into piled up structures as polar–nonpolar repulsion between assembled alkyl chains and the hydrophilic polysaccharide backbone. Non-covalent interactions are the main forces that hold supramolecular species together.[2] Despite its weak nature, relative to covalent interaction, when these interactions are used synergistically, a stable supramolecular complex could be formed. In this specific case, those interactions should create a synergistic effect and consequently are able to form and maintain a hollow structure with a wall thickness of around 16.7 µm that is shown in Fig. 7C. We have formulated a possible mechanism for the self-assembly of palmitoyl xanthan amphiphile (Fig. 8) into hollow capsular structures. The balance between charge repulsion and hydrophobic interaction in palmitoyl xanthan is sensitive to environmental pH and the presence of salts. In the absence of salts (water) the charge repulsion between the negatively charged carboxylic groups on xanthan is dominating. In PBS, the electrostatic repulsion resulting from the charged groups is suppressed by the accumulation of counter ions diffused from the PBS (screening effect), thus increasing the hydrophobic interaction.

3.10 Xanthan-palmitoyl microcapsule formation and cell encapsulation

When designing materials for cell encapsulation, several properties should be considered for cell optimum biological functions. For instance, the amount and the character of functional groups contained in monomer units will influence the intermolecular interactions and also the interactions that lead to the capsule formation. As mentioned previously, palmitoyl xanthan by itself in physiological conditions is able to form self-supporting capsules in the presence of ions which are stable over a long term. Although appropriate for cell encapsulation purposes, these capsules are not physically stable enough to enclose cells and protect from immunotoxins. For this reason, the PX(X = 1.7P) microcapsules, which have negatively charged carboxyl groups, were coated with cationic poly-L-lysine (PLL). The PLL is well studied in cell encapsulation and has showed satisfactory

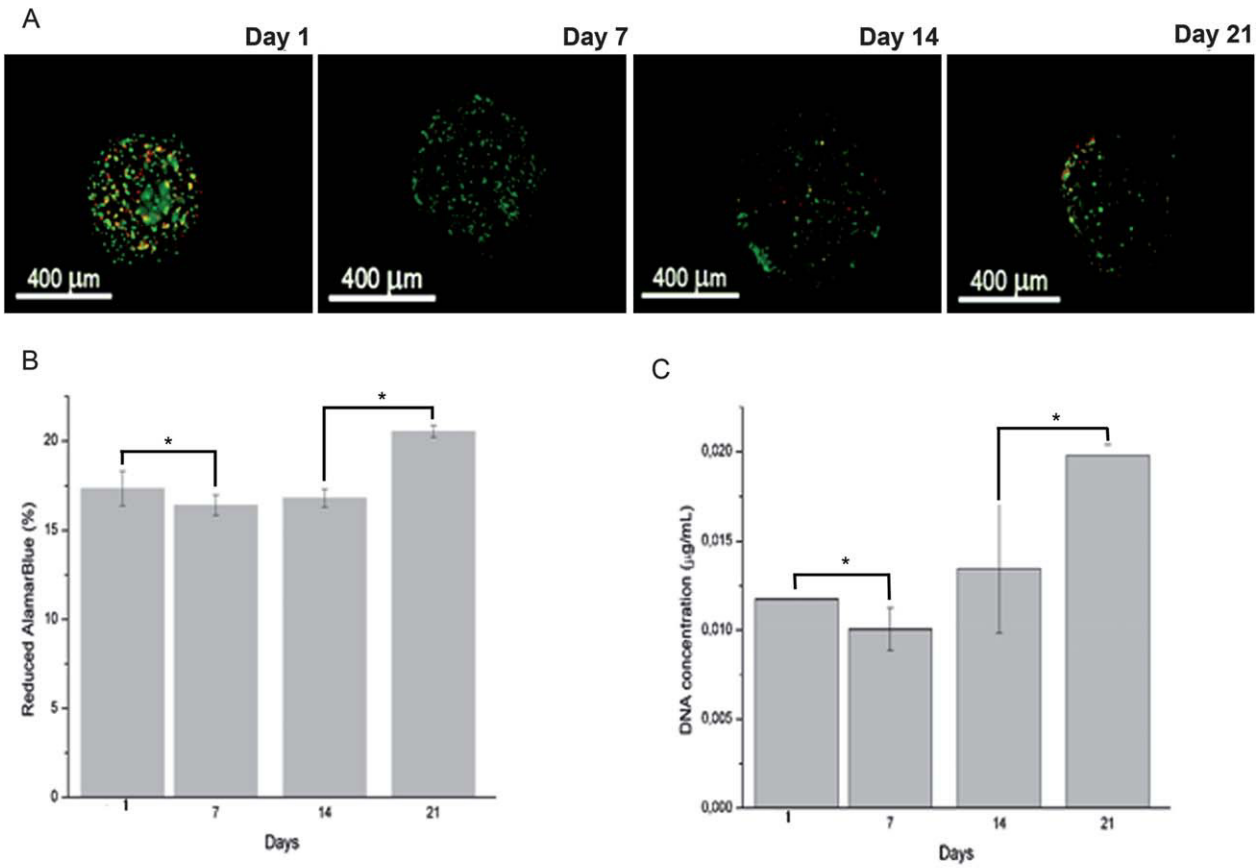

Fig. 10 *In vitro* viability and proliferation of ATDC5 cells cultured in PX(X = 1.70P)/PLL microcapsules. (A) Fluorescence microscopy images displaying the live/dead assay of encapsulated cells (green cells are live, red cells are dead) showing that the cells remain viable in the microcapsules up to 21 days of culture. (B) Metabolic activity and (C) proliferation of encapsulated cells determined by AlamarBlue® assay and DNA quantification. Results are expressed as means ± standard deviation with $n = 3$. * Indicates a significant difference ($p < 0.05$) for different time points.

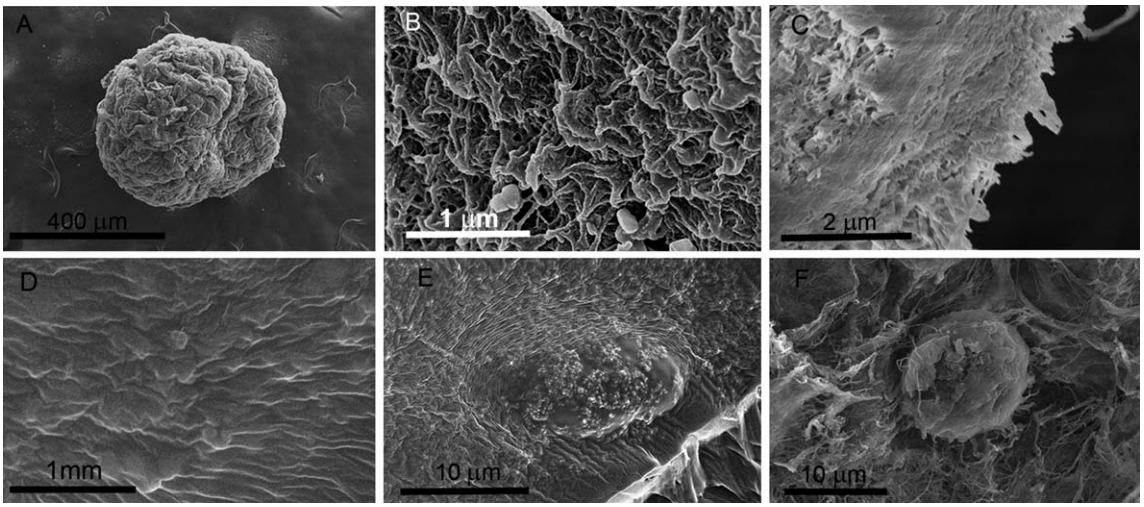

Fig. 11 SEM images showing the overall PX(X = 1.70P)/PLL microcapsule after 21 days of culture (A), the external surface (B) and the cross-section demonstrating the interface between PX(X = 1.70P) and poly-L-lysine complex (C). Internal surface (D) and morphological characteristics of the cells attached to the microcapsule inner surface (E) and (F).

performance in the encapsulation of cells with xanthan based material.[18] The microcapsules obtained in the present study were spherical and uniform in size with a diameter size around 576.6 ± 74 μm (Fig. 9).

3.11. *In vitro* viability, proliferation and morphology of ATDC5 cells cultured within microcapsules

To assess the ability of PX(X = 1.7P) microcapsules to sustain cell viability, we encapsulated ATDC5 cells, an immortalized chondrocytic cell line, within these self-assembled matrices. The morphology and viability of encapsulated cells in PX(X = 1.7P) microcapsules were investigated. Live/dead assay (Fig. 10A) shows that encapsulated cells remain viable up to 21 days of culture (viable cells depict a green fluorescence color), demonstrating the ability of palmitoyl xanthan self-assembled matrix to support cellular viability over prolonged time. Cell viability within the microcapsules is also confirmed by the results from the AlamarBlue® assay (Fig. 10B). Encapsulated cells were observed to reduce AlamarBlue® during 21 days of *in vitro* culture, exhibiting a slight increase in the metabolic activity from day 7 to day 21.

To validate the results from cell viability studies, cell proliferation was investigated by DNA quantification (Fig. 10C). A gradual increase in DNA concentration was observed from day 7 until day 21 as a result of improved cellular proliferation in PX(X = 1.7P) microcapsules.

Cell viability and proliferation within the microcapsules indicate that palmitoyl xanthan microcapsules are permeable as they are able to provide sufficient oxygen and nutrients necessary for cell survival and proliferation. The external surface was exposed to poly-L-lysine and it resulted in the fibrous network structure with porous appearance (Fig. 11B). SEM images of the microcapsule (Fig. 11B and D) reveal a fibrous outer layer and a denser inner layer can be appreciated. The inner surface of the microcapsule was comparatively smoother as it formed by the self-assembly process from diffused ions from external medium into the interior part of microdroplets in microcapsule formation (Fig. 11D). The cells were also detected to anchor tightly on the inner wall surface of the microcapsules as shown in Fig. 11E and F. Most mammalian cells are anchorage dependent and therefore have to adhere to a surface to express their optimum metabolic functionality and viability.[26] SEM analysis on cell cultured microcapsules after 21 days revealed that the cells were partially entrapped on the internal side of the dense microcapsule wall (Fig. 11E and F). This may be explained by the fact that nutrients and oxygen are more readily available at the capsule surface than in the microcapsule core. These core–shell type microcapsules, with partial embedding of cells on the inner wall, might be superior to cell microencapsulation into firm gels, like into alginate beads formed by ionic crosslinking, since the cells immobilized in the center of the gel would present decreased metabolic activity and proliferation as the diffusion of nutrients and oxygen would be more challenging at this location.

4. Conclusions

Palmitoyl xanthan with various conjugation ratios was successfully synthesized to obtain an amphiphilic polysaccharide. The amphiphilic character imparted to native xanthan only by a certain palmitoyl ratio allows the self-assembly into stable hollow capsule structures in cell-friendly conditions, *i.e.*, in the presence of physiological ion concentration and pH. Microcapsules with long-term stability and ability to support cell viability and proliferation *in vitro* over prolonged time were obtained using this self-assembling system. In summary, we have demonstrated the use of self-assembly to provide triggered activation for capsule formation. This approach provides an easy and versatile strategy for the construction of synthetic matrices capable of encapsulating living cells that could be applied in cell-delivery therapies.

Acknowledgements

This work was supported by the European Union funded project "Find and Bind" (NMP4-SL-2009-229292) under FP7. A. C.

Mendes thanks the Portuguese Foundation for Science Technology for a PhD grant (SFRH/BD/42161/2007). We thank Emanuel Fernandes of the 3B's Research Group at the University of Minho for his assistance with DSC analysis.

References

1 P. Chen, *Colloids Surf., A*, 2005, **261**, 3–24.
2 D. R. T. Jonathan, W. Steed, K. J. Wallace, in *Core Concepts in Supramolecular Chemistry and Nanochemistry*, ed. J. W. Sons, 1969.
3 D. W. P. M. Lowik, E. H. P. Leunissen, M. van den Heuvel, M. B. Hansen and J. C. M. van Hest, *Chem. Soc. Rev.*, 2010, **39**, 3394–3412.
4 K. Akiyoshi, E. C. Kang, S. Kurumada, J. Sunamoto, T. Principi and F. M. Winnik, *Macromolecules*, 2000, **33**, 3244–3249.
5 J. D. Hartgerink, E. R. Zubarev and S. I. Stupp, *Curr. Opin. Solid State Mater. Sci.*, 2001, **5**, 355–361.
6 C. Duval-Terrié, J. Huguet and G. Muller, *Colloids Surf., A*, 2003, **220**, 105–115.
7 G. K. Bourov and A. Bhattacharya, *J. Chem. Phys.*, 2005, **122**, 1–6.
8 K. Akiyoshi and J. Sunamoto, *Supramol. Sci.*, 1996, **3**, 157–163.
9 C. Rouzes, A. Durand, M. Leonard and E. Dellacherie, *J. Colloid Interface Sci.*, 2002, **253**, 217–223.
10 J. Cheng, J.-b. Zhu, N. Wen and F. Xiong, *Int. J. Pharm.*, 2006, **313**, 136–143.
11 J. S. Rodrigues, N. S. Santos-Magalhães, L. C. B. B. Coelho, P. Couvreur, G. Ponchel and R. Gref, *J. Controlled Release*, 2003, **92**, 103–112.
12 C. Rouzes, M. Leonard, A. Durand and E. Dellacherie, *Colloids Surf., B*, 2003, **32**, 125–135.
13 C. Schorsch, C. Garnier and J.-L. Doublier, *Carbohydr. Polym.*, 1995, **28**, 319–323.
14 I. Capron, G. Brigand and G. Muller, *Polymer*, 1997, **38**, 5289–5295.
15 B. Katzbauer, *Polym. Degrad. Stab.*, 1998, **59**, 81–84.
16 F. García-Ochoa, V. E. Santos, J. A. Casas and E. Gómez, *Biotechnol. Adv.*, 2000, **18**, 549–579.
17 M. Hamcerencu, J. Desbrieres, M. Popa, A. Khoukh and G. Riess, *Polymer*, 2007, **48**, 1921–1929.
18 A. C. Mendes, E. T. Baran, R. C. Pereira, H. S. Azevedo and R. L. Reis, submitted.
19 G.-B. Jiang, D. Quan, K. Liao and H. Wang, *Carbohydr. Polym.*, 2006, **66**, 514–520.
20 E. T. Baran, A. C. Mendes, H. S. Azevedo and R. L. Reis, *Portuguese pat.*, (105489).
21 G. K. Prakash and K. M. Mahadevan, *Appl. Surf. Sci.*, 2008, **254**, 1751–1756.
22 Y.-L. Chiu, S.-C. Chen, C.-J. Su, C.-W. Hsiao, Y.-M. Chen, H.-L. Chen and H.-W. Sung, *Biomaterials*, 2009, **30**, 4877–4888.
23 R. Benages, L. Bayes, R. Cordobilla, E. Moreno, T. Calvet and M. A. Cuevas-Diarte, *Cryst. Growth Des.*, 2009, **9**, 1762–1766.
24 R. P. Millane and B. Wang, *Carbohydr. Polym.*, 1990, **13**, 57–68.
25 T. Lim, J. T. Uhl and R. K. Prud'homme, *J. Rheol.*, 1984, **28**, 367–379.
26 S. R. Bhatia, S. F. Khattak and S. C. Roberts, *Curr. Opin. Colloid Interface Sci.*, 2005, **10**, 45–51.

